Available online at www.sciencedirect.com
ScienceDirect
Journal of Sound and Vibration 305 (2007) 289–297
JOURNAL OF SOUND AND VIBRATION
www.elsevier.com/locate/jsvi

Short Communication

Concerning the cause of instability in time-stepping boundary element methods applied to the exterior acoustic problem

H. Wang[a,*], D.J. Henwood[b], P.J. Harris[b], R. Chakrabarti[b]

[a] *College of Physical and Environmental Oceanography and Physical Oceanography Laboratory, Ocean University of China, Qingdao 266100, PR China*
[b] *School of Computing and Mathematical Sciences, University of Brighton, Lewes Road, Moulsecoomb, Brighton BN2 4GJ, UK*

Received 23 October 2005; received in revised form 11 May 2006; accepted 3 March 2007

Abstract

The boundary element method (BEM) in its simple form when solving the exterior acoustic problem in the frequency domain has difficulties at the frequencies of internal resonances of the closed structure. The corresponding time domain form of the exterior problem often exhibits instabilities in the time-stepping process. The link between these two features is investigated by relating the eigenvalues of the iterating matrix of the time-stepping process to damped frequencies. Numerical evidence from a problem with an analytic solution, and from a loudspeaker response are given. The suggested link implies that instability comes from numerical errors super-imposed on a more fundamental problem and may be best tackled through a time domain technique corresponding to the methods already available in the frequency domain.

1. Introduction

The background concern of this short communication is the numerical prediction of the excess acoustic pressure, ϕ, exterior to a closed vibrating surface in both the time and frequency domains. Working in the time domain requires solving the (linear) wave equation, and the instability referred to is the result of matrix iteration in time-stepping and shows up in the time solution as an increasing response developing after a period of quiet—even though no excitation is applied. The discussion is not directly relevant to general element methods in other contexts such as the nonlinear transient analysis of engineering structures.

A common method of solving the exterior acoustic problem in the frequency domain is by using Helmholtz' equation, converting to a boundary integral equation (BIE) and then applying an element discretisation, to become the boundary element method (BEM). A well-known difficulty in the simplest form of the BEM occurs at the set of frequencies at which the interior homogeneous problem has non-zero solutions, [1]. These frequencies are referred to in this communication as f_d. Various methods for creating a modified equation with a solution at all frequencies have been devised, e.g. Ref. [1], or the CHIEF method of Schenck [2]. Without a modified form the BEM cannot be relied on, since it is not possible to predict in advance where the

*Corresponding author. Tel.: +860 13506424330.
E-mail address: wanghui2@ouc.edu.cn (H. Wang).

0022-460X/$ - see front matter
doi:10.1016/j.jsv.2007.03.083

frequencies f_d occur for a general structure. The modified form has led to an acceptably robust method for the exterior problem up to a reasonably high frequency.

The inverse Fourier transform applied to the BIE gives the time domain version, referred to as the retarded potential integral equation (RPIE), which when discretised leads to a time-stepping scheme. Instability is well known and an analysis of various averaging methods to stabilise the process is given by Davies and Duncan [3]. Walker et al. [4] discusses stability through the eigenvalues of an single iterative matrix, see Section 3 of this paper, but do not make the link with internal resonances which we see as crucial. The connection between instability and internal resonances in scattering problems has been recognised, e.g. Refs. [5,6]. Smith suggested that it could be rectified by an averaging of the time steps; Ergin advocates the more radical action of modifying of the RPIE by the Burton and Miller method which seems to us to be a better approach, going to the heart of the problem. Although acoustics is mentioned in the papers, the connection between internal resonances and instability has not been generally recognised in exterior acoustic problems.

Numerical evidence is given to establish the link through relating each eigenvalue of an iterative matrix with a particular frequency. The implication of the link on attempting to find a cure for instability is examined.

2. The exterior problem in the frequency domain

Helmholtz' equation is converted into a BIE by introducing a fundamental solution, G, of Helmholtz' equation (commonly called Green's function). In three dimensions G at frequency ω is given by

$$G_k(\mathbf{p},\mathbf{q}) = \frac{1}{4\pi R}\exp(\mathrm{j}kR), \quad \mathrm{j} = \sqrt{-1}, \tag{1}$$

where the wavenumber $k = \omega/c$, c is the speed of sound, and $R = |\mathbf{p}-\mathbf{q}|$ is the distance between a (source) point on the surface $\mathbf{q}$ and the (observation) point $\mathbf{p}$.

Omitting details, which may be found in many sources, e.g. Ref. [1], G_k and ϕ are combined into an integral equation for ϕ at $\mathbf{p}$,

$$\alpha\phi(\mathbf{p},\omega) = \int_S \left\{ \phi(\mathbf{q},\omega)\frac{\partial G_k(\mathbf{p},\mathbf{q})}{\partial \mathbf{n}_q} - G_k(\mathbf{p},\mathbf{q})\frac{\partial \phi(\mathbf{q},\omega)}{\partial \mathbf{n}_q} \right\} \mathrm{d}S_q. \tag{2}$$

Here S is the smooth surface of a structure and

$$\alpha = \begin{cases} 1 & \text{if } \mathbf{p} \text{ is in the exterior,} \\ 1/2 & \text{if } \mathbf{p} \text{ is on } S, \\ 0 & \text{if } \mathbf{p} \text{ is in the interior.} \end{cases}$$

The normal derivative $\partial\phi/\partial\mathbf{n}_q = v$ is the given surface condition.

The BEM discretises Eq. (2), for each k, into

$$\alpha\phi(\mathbf{p}) = \mathbf{m}_k\boldsymbol{\phi} - \mathbf{l}_k\mathbf{v}, \tag{3}$$

where $\boldsymbol{\phi}$, $\mathbf{v}$ are vectors of the values of ϕ, v at chosen points (nodes) on the boundary, and $\mathbf{m}_k, \mathbf{l}_k$ are vectors computed from integrating G_k with chosen element shape functions on the boundary elements. (In the numerical evidence shown later, the simplest, constant approximation, was used and the nodes were chosen at the element mid-points.)

The boundary condition supplies $\mathbf{v}$; $\boldsymbol{\phi}$ is calculated by applying the collocation method to Eq. (3) bringing $\mathbf{p}$ to each node in turn. This is the initial stage of the BEM and is the significant part of the BEM needed for the discussion of instability in the time domain (the final stage is to again apply Eq. (3), where now $\mathbf{p}$ is a general point in the exterior, but this will not concern us). The initial stage has a matrix form

$$(M_k - \tfrac{1}{2}I)\boldsymbol{\phi} = L_k\mathbf{v}, \tag{4}$$

where M_k, L_k are computed similarly to $\mathbf{m}_k, \mathbf{l}_k$.

There is a difficulty in solving Eq. (4) in that $(M_k - \frac{1}{2}I)$ is singular at the set of frequencies, f_d, mentioned earlier.

3. The exterior problem in the time domain

The inverse Fourier transform applied to Eq. (2) gives the time domain version. As a result of G being frequency dependent, as shown in Eq. (1), it becomes modified into causing a time delay. Again omitting details of the well-established derivation, see e.g. Ref. [7]

$$\alpha\phi(\mathbf{p},t) = -\frac{1}{4\pi}\int_S \left\{ \frac{1}{R^2}\frac{\partial R}{\partial \mathbf{n}_q}\left[\phi(\mathbf{q},\tau) + \frac{R}{c}\frac{\partial\phi(\mathbf{q},\tau)}{\partial t}\right] + \frac{1}{R}\frac{\partial\phi(\mathbf{q},\tau)}{\partial \mathbf{n}_q} \right\} \mathrm{d}S_q, \tag{5}$$

where $\tau = t - (R/c)$ is the retarded time at which sound must start out at $\mathbf{q}$ in order to reach $\mathbf{p}$ at time t. The computation is divided into two stages in a similar manner to the frequency domain version. The first stage is to obtain the initially unknown ϕ at the chosen nodal points on the surface, before using them to obtain ϕ at an exterior point.

Eq. (5) is discretised into a set of linear equations, which is similar with the frequency domain Eq. (2) except that the pressure over a structure at a sequence of time levels is needed in order to advance the solution through one time step. Details are given in Ref. [8].

In order to predict the time behaviour in the exterior region the boundary pressures on the surface have to be predicted in the same way that Eq. (4) has to be used before Eq. (3) in the frequency domain. The time domain form of Eq. (4) is

$$\boldsymbol{\phi}_i = \sum_{n=1}^{\mathrm{N}} D^{(n)}\boldsymbol{\phi}_{i-n} + \mathbf{y}_i. \tag{6}$$

The vector $\boldsymbol{\phi}_i$ contains the values of ϕ at the M chosen nodal points and at the time $i\Delta t$. Δt is a suitably chosen time step, and i is the iteration count. The number of time steps required to progress the computation to the next time level is N, where $N\Delta t$ just covers the time interval needed for sound from the point on S furthest from $\mathbf{p}$ to reach $\mathbf{q}$. The matrices $D^{(n)}$ come from the BEM, for details see Ref. [8]. Finally, $\mathbf{y}_i$ comes from the given boundary values of $\partial\phi/\partial\mathbf{n}_q$.

This is the usual form given in the literature [9], but for the purposes of analysing stability, this may be written as a (large) iterative scheme:

$$\mathbf{\Phi}_i = H\mathbf{\Phi}_{i-1} + \mathbf{g}_i, \tag{7}$$

where

$$\mathbf{\Phi}_i = \begin{bmatrix} \boldsymbol{\phi}_{i-\mathrm{N}+1} \\ \boldsymbol{\phi}_{i-\mathrm{N}+2} \\ \vdots \\ \boldsymbol{\phi}_{i-1} \\ \boldsymbol{\phi}_i \end{bmatrix}, \quad H = \begin{bmatrix} \mathbf{0} & I & \mathbf{0} & \dots & \mathbf{0} \\ \mathbf{0} & \mathbf{0} & I & \dots & \mathbf{0} \\ \vdots & \vdots & \vdots & \ddots & \vdots \\ \mathbf{0} & \mathbf{0} & \mathbf{0} & \dots & I \\ D^{(\mathrm{N})} & D^{(\mathrm{N}-1)} & D^{(\mathrm{N}-2)} & \dots & D^{(1)} \end{bmatrix}, \quad \mathbf{g}_i = \begin{bmatrix} \mathbf{0} \\ \mathbf{0} \\ \vdots \\ \mathbf{0} \\ \mathbf{y}_i \end{bmatrix}. \tag{8}$$

The first $M-1$ rows merely state that $\boldsymbol{\phi}_i = \boldsymbol{\phi}_i$, and the last repeats Eq. (6). Multiplying by the matrix H upgrades a set of surface values of ϕ at the structure node points, $1, 2, \dots M$, and at the set of times $(i-N)\Delta t, (i-N+1)\Delta t, \dots (i-1)\Delta t$. In particular the homogeneous case where $\mathbf{g}_i = \mathbf{0}$, i.e. after the forcing function has ceased to act, will be considered.

$$\mathbf{\Phi}_i = H\mathbf{\Phi}_{i-1}. \tag{9}$$

4. A look at the structure of the eigensystem of H

A single, representative eigenvalue and corresponding eigenvector are considered in order to examine the step-wise propagation in time. The results will be relevant for the eigensystem as a whole and since collectively they form a basis for the solution from any start, they will inform about the general solution of the homogeneous equation.

Suppose $\lambda = r\exp(\mathrm{j}\theta)$ and $\mathbf{U}$ are an eigenvalue and vector of the iterative matrix H, i.e.

$$H\mathbf{U} = \lambda\mathbf{U}. \tag{10}$$

Following the $NM \times 1$ vector structure of $\mathbf{\Phi}$ described in Eq. (8), $\mathbf{U}$ may be partitioned into N sets of M element values,

$$\mathbf{U}^{\mathrm{T}} = [\mathbf{u}_1^{\mathrm{T}}, \mathbf{u}_2^{\mathrm{T}}, \ldots \mathbf{u}_{\mathrm{N}}^{\mathrm{T}}],$$

where $\mathbf{u}_i$ is a set of nodal values at a fixed time, $i\Delta t$. In full this is

$$\begin{bmatrix} \mathbf{0} & I & \mathbf{0} & \ldots & \mathbf{0} \\ \mathbf{0} & \mathbf{0} & I & \ldots & \mathbf{0} \\ \vdots & \vdots & \vdots & \ddots & \vdots \\ \mathbf{0} & \mathbf{0} & \mathbf{0} & \ldots & I \\ D^{(\mathrm{N})} & D^{(\mathrm{N}-1)} & D^{(\mathrm{N}-2)} & \ldots & D^{(1)} \end{bmatrix} \begin{bmatrix} \mathbf{u}_1 \\ \mathbf{u}_2 \\ \vdots \\ \mathbf{u}_{\mathrm{N}-1} \\ \mathbf{u}_{\mathrm{N}} \end{bmatrix} = \lambda \begin{bmatrix} \mathbf{u}_1 \\ \mathbf{u}_2 \\ \vdots \\ \mathbf{u}_{\mathrm{N}-1} \\ \mathbf{u}_{\mathrm{N}} \end{bmatrix}. \tag{11}$$

From the matrix rows of Eq. (11)

$$\mathbf{u}_2 = \lambda\mathbf{u}_1, \mathbf{u}_3 = \lambda\mathbf{u}_2 = \lambda^2\mathbf{u}_1, \ldots, \mathbf{u}_{\mathrm{N}} = \lambda\mathbf{u}_{\mathrm{N}-1} = \lambda^{\mathrm{N}-1}\mathbf{u}_1$$

and the last row is

$$D^{(\mathrm{N})}\mathbf{u}_1 + D^{(\mathrm{N}-1)}\mathbf{u}_2 + \cdots + D^{(1)}\mathbf{u}_{\mathrm{N}} = \lambda\mathbf{u}_{\mathrm{N}}.$$

The left-hand side of this equation, using the definition of Eq. (6) with $\mathbf{y}_i = \mathbf{0}$, forms the set of boundary pressures at the next time level, say $\mathbf{u}_{\mathrm{N}+1}$.

Thus two successive pressure sets with the form of $\mathbf{\Phi}$ are

$$\mathbf{U}_{i-1} = \begin{bmatrix} \mathbf{u}_1 \\ \mathbf{u}_2 \\ \vdots \\ \mathbf{u}_{\mathrm{N}-1} \\ \mathbf{u}_{\mathrm{N}} \end{bmatrix}, \quad \mathbf{U}_i = \begin{bmatrix} \mathbf{u}_2 \\ \mathbf{u}_3 \\ \vdots \\ \mathbf{u}_{\mathrm{N}} \\ \mathbf{u}_{\mathrm{N}+1} \end{bmatrix} = \lambda \begin{bmatrix} \mathbf{u}_1 \\ \mathbf{u}_2 \\ \vdots \\ \mathbf{u}_{\mathrm{N}-1} \\ \mathbf{u}_{\mathrm{N}} \end{bmatrix},$$

i.e. satisfy

$$\mathbf{U}_i = H\mathbf{U}_{i-1} = \lambda\mathbf{U}_{i-1}. \tag{12}$$

This implies that from $\mathbf{u}_1$ the pressures at subsequent times may be generated by the simple iteration

$$\mathbf{u}_i = \lambda\mathbf{u}_{i-1}. \tag{13}$$

Let

$$\mathbf{u}_1 = [b_1\exp(\mathrm{j}\alpha_1), b_2\exp(\mathrm{j}\alpha_2), \ldots, b_M\exp(\mathrm{j}\alpha_M)]^{\mathrm{T}}, \tag{14}$$

then

$$\mathbf{u}_{i+1} = \lambda^i\mathbf{u}_1 = r^i[b_1\exp\mathrm{j}(\alpha_1 + i\theta), b_2\exp\mathrm{j}(\alpha_2 + i\theta), \ldots, b_M\exp\mathrm{j}(\alpha_M + i\theta)]^{\mathrm{T}}. \tag{15}$$

Note that, since H is real, the eigenvalues and vectors either real or occur in conjugate pairs, so real pressures may be taken from the real or imaginary part of Eq. (15),

$$r^i[b_1\cos(\alpha_1 + i\theta), b_2\cos(\alpha_2 + i\theta), \ldots, b_M\cos(\alpha_M + i\theta)]^{\mathrm{T}}$$
$$\text{or } r^i[b_1\sin(\alpha_1 + i\theta), b_2\sin(\alpha_2 + i\theta), \ldots, b_M\sin(\alpha_M + i\theta)]^{\mathrm{T}}.$$

5. The time eigensystem related to frequencies

Eq. (15) shows that the effect of progressing through a time step Δt is to move the vector through an angle θ i.e.

$$\begin{aligned} &\text{at a rate of } \frac{\theta}{\Delta t} \text{ radians per second} \\ &\text{or } \frac{\theta}{2\pi\Delta t} \text{ Hz} \\ &\text{or wavenumber } \frac{\theta}{c\Delta t}, \end{aligned}$$

where c is the speed of sound. In this way a picture of the eigenvalues may be shown either as complex numbers, see Fig. 1, or alternatively in a frequency form shown in Fig. 2. The values in the illustration come from the problem with an analytic solution, described in Section 6.1. In the frequency form the y-axis is used for the decay rate, r, which in the polar plot becomes the radius.

The association of eigenvalues with frequencies may be obtained more formally by considering the effect of the Fourier transform on the sequence of vectors produced by the iterative scheme. From Eq. (13) and the start of $\mathbf{u}_1$, the sequence

$$\mathbf{u}_1, \lambda\mathbf{u}_1, \lambda^2\mathbf{u}_1, \lambda^3\mathbf{u}_1, \ldots$$

is produced. Let this be $h_i\mathbf{u}_1, i = 0, 1, 2, \ldots$, where $h_i = \lambda^i = [r\exp(\mathrm{j}\theta)]^i$ contains the variation with time and $\mathbf{u}_1$ is constant through the iteration process. At this stage we assume that $r<1$. Since the times $i\Delta t$ may be thought of as samples from continuous time t, h_i is sampled data from the continuous function

$$\begin{aligned} h(t) &= [r\exp(\mathrm{j}\theta)]^{t/\Delta t} \\ &= [\exp(-\alpha + \mathrm{j}\theta)]^{t/\Delta t} \quad \text{where } \alpha = -\ln r \\ &= \exp\left[\left(-\frac{\alpha}{\Delta t} + \mathrm{j}\frac{\theta}{\Delta t}\right)t\right] \\ &\text{defining } \hat{f} \text{ as } \theta/(2\pi\Delta t) \text{ and } \beta \text{ as } \alpha/\Delta t \\ &= \exp(-\beta + \mathrm{j}2\pi\hat{f})t. \end{aligned}$$

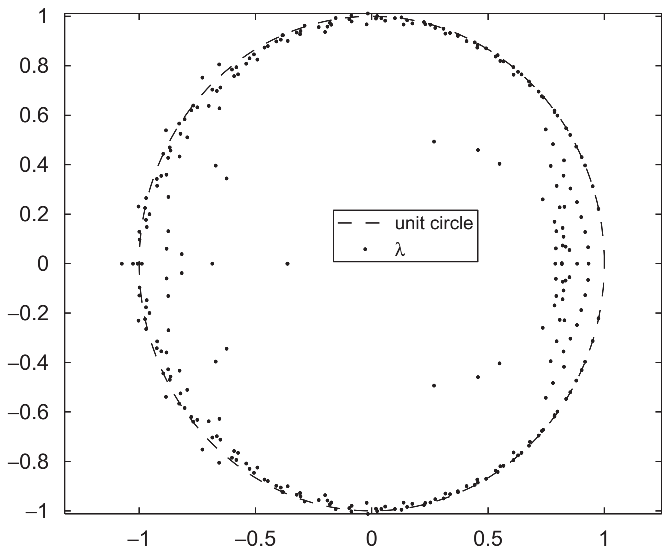

Fig. 1. Polar form (r, θ) of the eigenvalues λ.

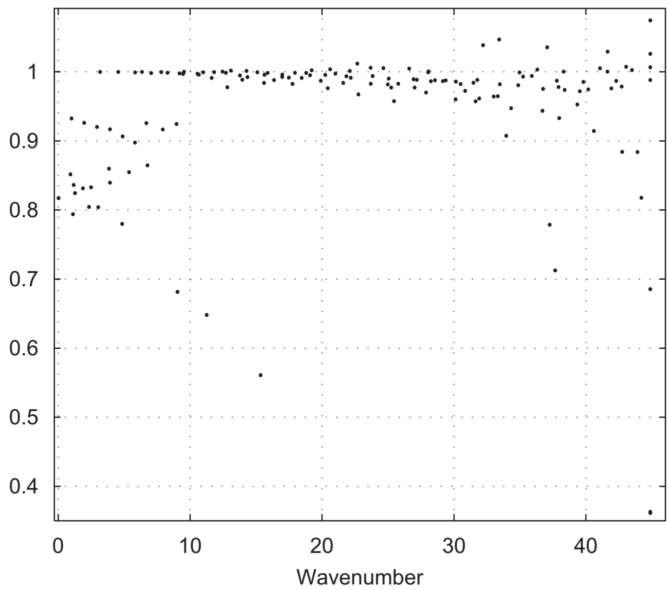

Fig. 2. Frequency form of the eigenvalues with the decay factor r on the y-axis and $\theta/c\Delta t$ on the x-axis.

The Fourier transform is

$$\begin{aligned} H(f) &= \int_{-\infty}^{\infty} h(t)\exp(-\mathrm{j}2\pi f t)\,\mathrm{d}t \\ &= \int_{0}^{\infty} \exp(-\beta + \mathrm{j}2\pi\hat{f})t\exp(-\mathrm{j}2\pi f t)\,\mathrm{d}t \\ &= \int_{0}^{\infty} \exp(-\beta + \mathrm{j}2\pi(\hat{f} - f))t\,\mathrm{d}t \\ &= \frac{1}{\beta - \mathrm{j}2\pi(\hat{f} - f)}. \end{aligned} \tag{16}$$

A graph of the modulus of $H(f)$ is shown in Fig. 3 for the particular example $\hat{f} = 100\,\mathrm{Hz}$ and for varying β. Note that r is related to β by

$$r = \exp(-\Delta t\beta) \text{ so that } \beta \to 0 \Rightarrow r \to 1.$$

The appearance is of a typical damped resonance at 100 Hz.

Notes: The first two notes explain the effect of using discrete samples of $h(t)$ rather than the continuous function.

1. The Nyquist criteria [10], which requires at least two sample points per cycle, is relevant here. The corresponding highest frequency is $f_c = 1/(2\Delta t)$. That the frequency $\hat{f}$ should be constrained in this way requires that

$$\hat{f} < \frac{1}{2\Delta t} \Rightarrow \frac{\theta}{(2\pi\Delta t)} < \frac{1}{2\Delta t} \text{ or } \theta < \pi. \tag{17}$$

This removes an ambiguity in forming θ from the complex number λ (both θ and $-\theta$ occur as the eigenvalues are in conjugate pairs).

As θ increases from zero to π the corresponding frequency increases from zero to the Nyquist value f_c.

2. The sampled frequencies resulting from the sampled time data have frequency step of $1/N\Delta t$, see Ref. [10]. Thus they may not include exactly the damped resonance at $\hat{f}$ derived from the eigenvalue. Consequently even if $\hat{f}$ is exactly a member of f_d the discrete frequency data may not fall on the member of f_d.

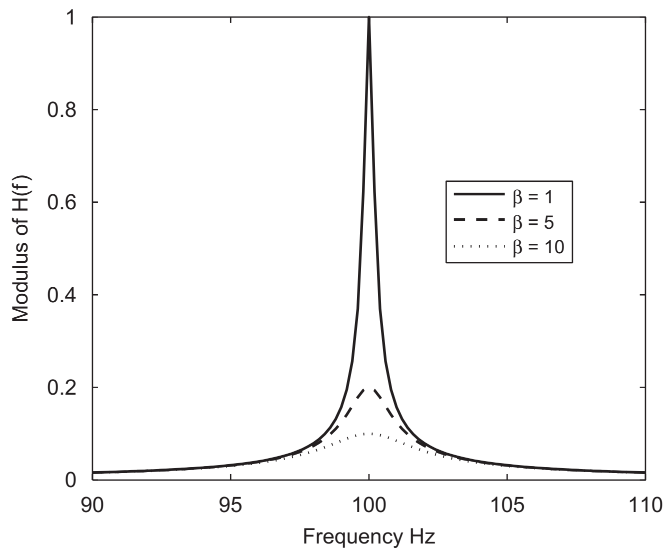

Fig. 3. Showing the modulus of the Fourier transform, $H(f)$ for $\hat{f} = 100$.

3. If $r = 1$ the amplitude of the oscillation does not decay but remains constant, which is clearly an undamped resonance.

In Eq. (16) $|H(f)|$ has its largest value (the surface resonates) at $2\pi f \Delta t = \theta$, i.e. $f = \theta/2\pi\Delta t$ as before. Note that as $r \to 1$, $|H(f)| \to \infty$ and for r near 1 it has the appearance of an undamped resonance.

We suggest that the frequencies of these resonances are members of f_d. Also that the eigenvalues of H which have modulus ≈ 1 come from these undamped resonances $r = 1$ but are affected by averaging, rounding, or numerical integration error.

Clearly if $r > 1$ the iteration process will be unstable and if $r < 1$ then stable. A small change in r when $r \approx 1$ may tip a resonance over from being stable to unstable or vice versa.

In the next section numerical evidence is given to confirm the suggestion. The statement that " $r \approx 1$" is not precise in that no indication is given of how close to 1 is intended, but the message from the evidence is clear.

6. Numerical evidence that the frequencies having $r \approx 1$ are contained in f_d

In all cases the boundary elements used to generate the 3D surfaces were axi-symmetric hoops generated by straight line segments, and the pressure is assumed to be constant on each element.

6.1. An example with an analytical solution

The number of nodes (elements) was $M = 10$, and $\Delta t = 0.07$.

The analytic problem concerns the vibrating surface of a unit sphere with c taken as 1; the method of separation of variables gives as basis functions, for a problem with symmetry in the φ direction,

$$u_m(r,\theta) = P_m(\cos\theta) J_m(kr), \quad m = 0, 1, 2, \ldots .$$

Here θ is the angular variation giving the mode shape and r is the polar. P_m, J_m are the Legendre polynomial and spherical Bessel function of the first kind, of order m. For the homogeneous interior Dirichlet problem (our case) the solutions are given by the zeros of $J_m(ka)$ where a is the radius of the sphere; these are examples of f_D. Values are given in Ref. [11, pp. 467/8]. The first two are:

$$m = 0, \quad k = 3.1416\ (\pi), \quad P_0 = \text{constant},$$
$$m = 1, \quad k = 4.4934, \quad P_1 = \cos\theta.$$

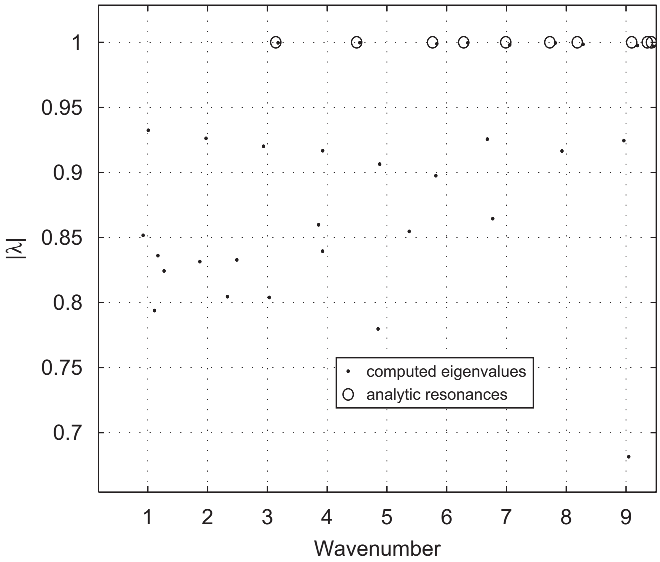

Fig. 4. Showing the analytic f_d on a plot of the eigenvalues.

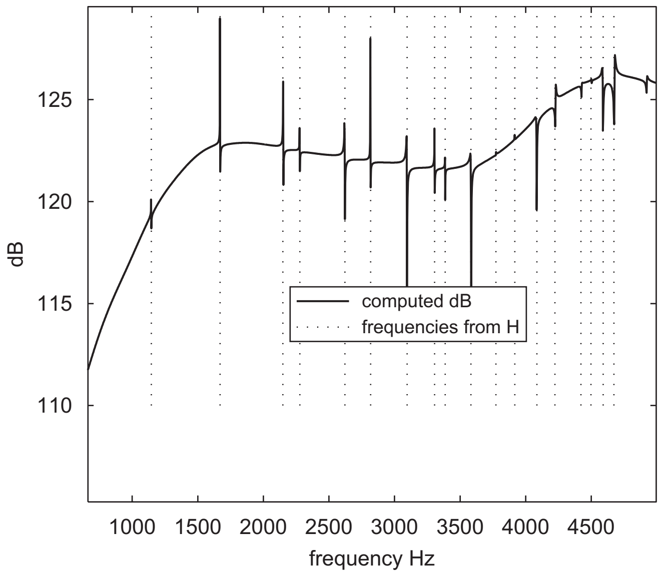

Fig. 5. Showing the simple form of frequency response of a loudspeaker together of the eigenvalues of the time solution.

Fig. 4 is a magnified section of Fig. 2 with the analytic resonances added and indicated by circles. There is good correspondence for the range shown, though the accuracy decreases as the frequency increases. Note that only one computed eigenvalue in the range shown has modulus greater than one (the frequency ≈ 9.5). The eigenvector was also considered for the first two modes and they did correspond with the analytic shapes.

6.2. A loudspeaker model

The modelling of the exterior acoustic field from the vibration of a loudspeaker cone is used as a practical example. A paper cone, of outer radius 15 cm, is from a mid-range unit, the details of which are given in a conference paper [12]. Fig. 5 shows the simple BEM (without the Burton and Miller modification) estimation for the on axis sound pressure at 1.5 m from the cone. The interior resonances clearly show up. The time domain model uses 64 elements and $\Delta t = 0.00004$ to form H and its eigenvalues. The related frequencies are marked by dotted lines. Again the correspondence is convincing. The decibel measure of the pressure is given by

$$20^{*} \log 10((\text{abs}(\text{pressure}))/(2.0\text{e} - 5)).$$

7. Conclusions

Interior resonances of a vibrating structure have long been known to cause difficulties in using the BEM in solving the exterior acoustic problem in the frequency domain. Because the frequency and time domains are equivalent, this same difficulty must be present in the time domain solution with the RPIE method. This is confirmed in the communication through:

- Establishing that each eigenvalue of the iteration matrix of the discrete time solution is shown to relate to a frequency of the Fourier transform of the time data.
- Evidence is given that the interior acoustic resonant frequencies of a structure appear in the time solution.
- The interior resonances appear in the time solution as eigenvalues with, if computed exactly, decay rate = 1. However numerical approximations may cause the decay rate to be <1 or >1, resulting in stability or instability, respectively.

Rather than modifying the averaging process or time step, a more thorough approach to eliminating the possible instability is to obtain a set of basis functions for the solution space of the homogeneous solution which exclude the interior resonances, in a way related to the Burton and Miller or CHIEF method for the frequency domain.

Acknowledgements

We wish to thank B & W loudspeakers for their support of the research and Dr. G. Geaves for his advice. H. Wang's research work is supported by the National Basic Research Program of China (973 program, No. 2006CB400602) and Shandong Province Research Program (No. 2006BS08011).

References

[1] A.J. Burton, The solution of Helmholtz' equation in exterior domains using integral equations, NPL Report NAC, 30 January 1973.
[2] H.A. Schenck, Improved integral formulation for acoustic radiation problems, *Journal of the Acoustical Society of America* 44 (1) (1968) 41–58.
[3] P.J. Davies, D.B. Duncan, Averaging techniques for time-marching schemes for retarded potential integral equations, *Applied Numerical Mathematics* 23 (1997) 291–310.
[4] S.P. Walker, M.J. Bluck, I. Chatzis, The stability of integral equation time-domain computations for three-dimensional scattering; similarities and differences between electrodynamic and elastodynamic computations, *International Journal for Numerical Modelling-electronic Networks Devices and Fields* 15 (2002) 459–474.
[5] P.D. Smith, Instabilities in time marching methods for scattering: cause and rectification, *Electromagnetics* 10 (1990) 439–451.
[6] A.A. Ergin, B. Shanker, E. Michielssen, Analysis of transient wave scattering from rigid bodies using a Burton–Miller approach, *Journal of the Acoustical Society of America* 106 (5) (1999).
[7] C.A. Coulson, A. Jeffrey, *Waves: A Mathematical Approach to the Common Types of Wave Motion*, Longman Group Limited, London, 1977.
[8] H. Wang, Boundary Integral Modelling of Transient Wave Propagation with Application to Acoustic Radiation from Loudspeakers, Ph.D. Thesis, University of Brighton, 2004.
[9] P.J. Davies, Numerical stability and convergence of approximations of retarded potential integral equations, *SIAM Journal of Numerical Analysis* 31 (3) (1994) 856–875.
[10] W.H. Press, B.P. Flannery, S.A. Teukolsky, W.T. Vetterling, *Numerical Recipies*, Cambridge University Press, Cambridge, 1989, pp. 368–390.
[11] M. Abramowitz, I.A. Stegun, *Handbook of Mathematical functions*, Dover Publications, Inc., New york, 1972.
[12] D. Henwood, G. Geaves, Finite element modelling of a loudspeaker, part 1: theory and validation, *Presented at the 119th AES Convention*, New York, USA, 2005 October 7–10.